Journal of Mathematical Sciences: Advances and Applications
Volume 14, Number 1, 2012, Pages 1-16

NUMERICAL SIMULATION OF NORMAL STRESS DISTRIBUTION ON THE BASE OF GRANULAR PILES

WASEEM GHAZI ALSHANTI, BENCHAWAN WIWATANAPATAPHEE and Y. H. WU

Department of Mathematics
University of Ha'il
Ha'il
Saudi Arabia
e-mail: w.alshanti@uoh.edu.sa

Department of Mathematics
Faculty of Science
Mahidol University
Bangkok
Thailand
e-mail: scbww@mahidol.ac.th

Department of Mathematics and Statistics
Curtin University
Perth
Australia
e-mail: yhwu@maths.curtin.edu.au

Abstract

In this paper, we develop a mathematical model and numerical technique to investigate the distribution of the normal force on the base of granular piles. Two-dimensional discrete element (DEM) simulations, based on the soft

2010 Mathematics Subject Classification: 70F35, 82C05.

Keywords and phrases: particles, granular piles, numerical simulation.

Received November 7, 2011

particle contact model, have been carried out to generate granular piles by pouring granules from a rising funnel with a small outlet. The results show that the normal force distributions under the granular piles that constructed from localized source exhibit a local minimum at the centre of the base under the pile vertex. The results are in good agreement with experimental observations.

1. Introduction

At rest, granular materials possess a variety of mechanical properties, which cannot be projected on the basis of our experience with fluids or solids. One of these features is the distribution of the normal stress beneath a pile of granular materials. It is found that the stress distribution on the base of a granular pile depends on the way it is constructed. Moreover, although the normal stress acting on the base is generally considered to have the maximum value under the apex of the pile, it has been found that this is not necessarily always in the case. It was reported that the normal stress under the apex of the pile may have a local minimum called a *stress dip* which, however, is not a universal feature. Smid and Novosad [12] reported that such phenomenon may be attributed to the looseness of the deposition of particles, whereas the layers above the apex may have higher emptiness. Further experimental attempt was performed by Vanel et al. [13]. They investigated the effect of the construction history (depositional technique) of sandpile on the distribution of normal stresses along the base. The piles were formed either by pouring sand from a funnel with a small outlet or from large sieve (homogeneous rain). Localized sources yield the normal stress profile with a local minimum under the apex of the pile, while homogeneous rain profiles do not lead to stress dip. Many investigations have been carried out to investigate the "M" shape normal stress distribution such as those due to [10] and [11].

Continuum mechanical theory of granular materials has been used to investigate the horizontal and the normal force distributions. Although the problem of determination of the stress distribution on the base of a granular pile is famous, few analytic continuum mechanical approaches have been conducted. Aspects such as stress propagation and arch formation within a sand pile which, mainly, depend on the pile construction history

have been investigated via continuum theory [3, 4, 6, 9]. In 1997, Cantelaube and Goddard [2] proposed an elastoplastic model for the sandpile, which consists of an inner elastic region and an outer region at yield. More recently, Hill and Cox [7] proposed a new model for the sandpile, which consists of an inner dead region and an outer region at yield. In the other words, the authors in [7] solve the two-dimensional wedge stockpile problem, where the material is assumed to be entirely at yield.

As the existing continuum models do not give the "M" shape normal stress distribution as found in experiments, we establish a discrete element model and numerical algorithm to investigate the normal stress distribution on the base of the granular pile. The rest of the paper is organized as follows. In Section 2, the discrete element model and numerical algorithm are presented followed by the numerical simulation schemes. In Section 3, discussion of the numerical results is given with particular focus on the influences of particle size and pile height on the normal stress distribution. Finally, a conclusion is given in Section 4.

2. The DEM Model and Numerical Simulation Scheme

The present numerical simulations are based on the soft-particle discrete element method, which was originally proposed by Cundall and Strack [5]. In our simulation model, the granular particles are subjected; during simulation, to two types of forces including contact forces and gravitational force. The dynamic equations for the motion of each of the particles under the forces are

$$m_i \frac{d^2 r_i}{dt^2} = \sum_{j=1}^{N} F_{ij} + F_{ei}, \tag{1}$$

$$I_i \frac{d^2 \theta_i}{dt^2} = \sum_{j=1}^{N} M_{ij} + M_{ei}, \tag{2}$$

where m_i and I_i are the mass and the moment of inertia of particle i, $r_i(t)$ is the position vector of the centre of particle i, $\theta_i(t)$ is the rotational speed of particle i, F_{ei} and M_{ei} are external forces and moment, and F_{ij} is the contact force acting on particle i due to particle j. Unlike the gravitational body force, the particle contact forces act only when the particle is in contact with other particles and/or with a boundary wall. For any typical pair of particles i and j, if they are in contact, then the contact force is determined by the following formula:

$$F_{ij}(t) = F_{ijn}(t)\hat{n} + F_{ijs}(t)\hat{s}, \tag{3}$$

where $\hat{n}$ and $\hat{s}$ are unit vectors in the normal and shear directions of the contact plane, $F_{ijn}(t)$ and $F_{ijs}(t)$ denote, respectively, the magnitudes of the normal contact force and shear contact force. The normal contact force is determined by a damped linear spring model, while the tangential contact force is determined by a linear spring in series with a frictional sliding element model. The interaction forces developed between any two particles or between a particle and the boundary wall are calculated based on the physical properties and the relative velocities, namely,

$$F_{ijn}(t) = k_n H(\delta_{ijn}(t))\delta_{ijn}(t), \tag{4}$$

$$F_{ijs}(t) = -\operatorname{sign}\{\delta_{ijs}(t)\} \min\{k_s\delta_{ijs}(t),\ \mu F_{ijn}(t)\}, \tag{5}$$

where $\delta_{ijn}(t) = |r_i(t) - r_j(t)|$ is the normal compression and $\delta_{ijs}(t) = \int_0^t (\dot{r}_i(\eta) - \dot{r}_j(\eta)) \bullet s\, d\eta$ is the tangent displacement between particle i and j.

In order to reduce the number of contact checks for each particle, the neighbouring cell technique is implemented in the present simulations. Once the particle contact forces acting on a particle are calculated, the new velocity and position of the particle can be obtained by integrating the differential equations for particle motion over a small simulation time step.

Now, let $\nu_i = \dfrac{dr_i}{dt}$ and

$$z = \begin{bmatrix} r_1(t) \\ \theta_1(t) \\ r_2(t) \\ \theta_2(t) \\ \vdots \\ \theta_N(t) \end{bmatrix}, \quad \nu = \begin{bmatrix} \nu_1(t) \\ \omega_1(t) \\ \nu_2(t) \\ \omega_2(t) \\ \vdots \\ \omega_N(t) \end{bmatrix}, \quad p = \begin{bmatrix} F_1(t)/m_1 \\ M_1(t)/I_1 \\ F_2(t)/m_2 \\ M_2(t)/I_2 \\ \vdots \\ M_N(t)/I_N \end{bmatrix},$$

then the dynamics equations for the motion of the N particles can be written as

$$\frac{dz(t)}{dt} = \nu(t), \tag{6}$$

$$\frac{d\nu(t)}{dt} = p[x(t), \nu(t)], \tag{7}$$

which can be then solved by using a standard solver for systems of ordinary differential equations.

The input parameters in our simulations include: physical properties of the granular particles under consideration, initial conditions, and boundary conditions. The initial conditions include: the initial positions and velocities of all particles and the geometry of the boundary conditions. All parameters are non dimensionalized using the density of particle, gravitational acceleration, and particle diameter. The current simulations have been used to investigate the normal force distribution underneath granular piles constructed by pouring particles from a rising funnel with a small outlet. A list of used mechanical and environmental non-dimensional simulation parameters are given in Table 1.

Table 1. Normalized simulation parameters of granular pile construction

Parameter	Value (non-dimensional)
Number of particles, N_p	1000
Particle diameter, $_d / d_\circ$ (where $d_\circ$ = 1.0mm)	0.71-0.79 (uniform distribution)
Particle density, $\rho / \rho_\circ$ (where $\rho_\circ = 1.0 \times 10^2$mm)	1
Particle-particle normal spring stiffness, $K_{n,pp} / (\rho_\circ \bar{g} d_\circ^2)$	6.006×10^4
Particle-particle normal dashpot coefficient, $C_{n,pp} / (\rho_\circ \bar{g}^{0.5} d_\circ^{2.5})$	4.024×10^3
Particle-particle tangential spring stiffness, $K_{s,pp} / (\rho_\circ \bar{g} d_\circ^2)$	3.006×10^4
Particle-particle friction coefficient, μ_{pp}	1.0
Particle-wall normal spring stiffness, $K_{n,pw}$	6.006×10^4
Particle-wall normal dashpot coefficient, $C_{n,pw} / \rho_\circ (\bar{g}^{0.5} d_\circ^{2.5})$	2.01×10^4
Particle-wall tangential spring stiffness, $K_{s,pw} / (\rho_\circ \bar{g} d_\circ^2)$	3.006×10^4
Particle-wall friction coefficient, μ_{pw}	1.0
Gravity in x-direction, $\bar{g}_x / \bar{g}$	0.0
Gravity in y-direction, $\bar{g}_y / \bar{g}$	– 9.8
Time step, $\Delta t \sqrt{\bar{g} / d_\circ}$	5.2711×10^{-5}

It has been reported that the construction history affects the stress distribution at the bottom of a granular pile. In our simulations, we adopt the localized source method to construct granular piles. A funnel with a

10mm length outlet is used to pour particles onto a flat smooth but frictional wall with 300mm length. The funnel is placed above the horizontal base such that the initial distance between the funnel outlet and the horizontal wall is 20mm. The funnel under consideration is shown in Figure 1.

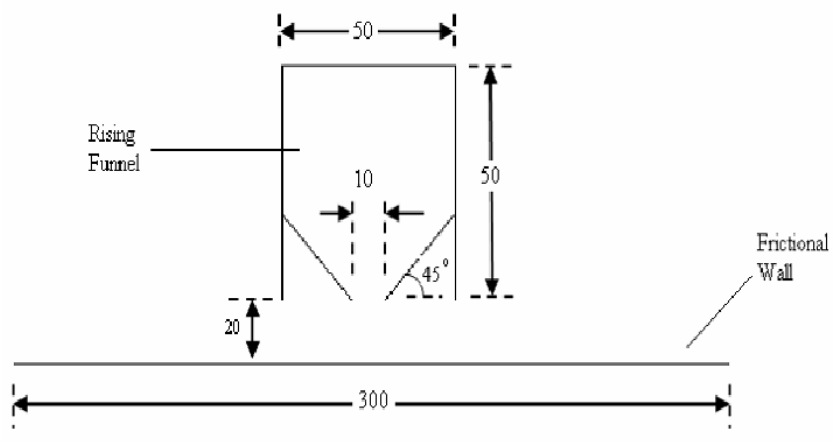

Figure 1. Non-dimensional funnel geometry.

To simulate a piling process, we firstly fill the funnel with particles completely, and then the funnel outlet is opened and the particles fall down under gravity onto the horizontal base. During the downward particle falling, the funnel moves upward with constant velocity. Due to the damping forces, the falling particles, eventually, come to rest and accumulate at the horizontal base forming a pile-like structure. The accumulative particles start to possess more height as more particles arrive at the apex of the pile and roll down the slopes and finally come to rest. Gradually, the height of the pile increases until it reaches the maximum height, when no more particles fall down from the funnel and all particles in the pile achieve a steady state condition as shown in Figure 2. To reduce the impact energy on the constructed pile, the crater funnel was kept close to the top of the growing pile. Over the total simulation time, the funnel horizontal position was constant and its crater was located directly above the top of the pile under construction.

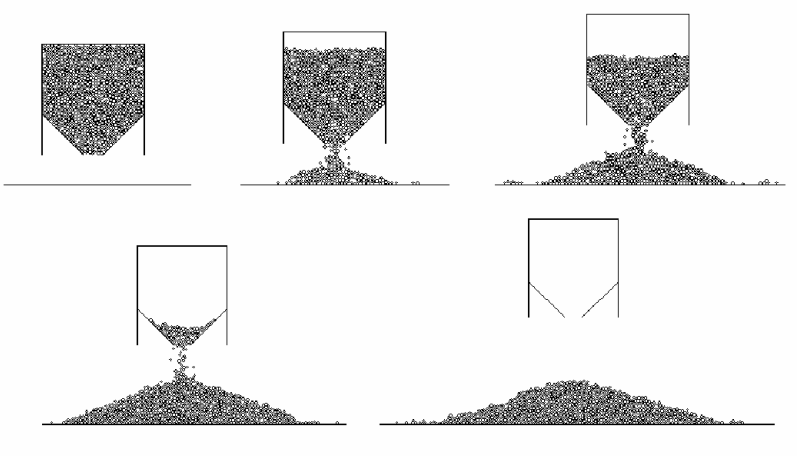

Figure 2. Consequential snapshots of the pile forming process.

During the piling process, two regions can be identified: inner (static) region and outer (dynamic) region as shown in Figure 3. For the inner region, the particles appear to achieve a static steady state, while particles of the outer region are not stable and roll down the slopes.

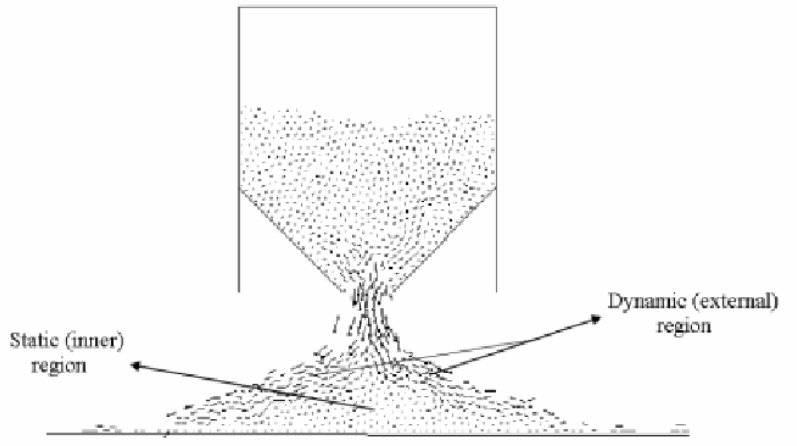

Figure 3. Dynamic and static regions during piling process.

To avoid errors, the normal stress distribution at the base of the granular pile was obtained at the final rest state, i.e., after the granular pile was given enough time to settle down and achieve a static steady state.

3. Simulation Results and Discussion

3.1. Influence of particle size

To study the effect of the particle size on the distribution of the normal force at the base of a granular pile, we conducted numerical simulations to construct two mono-sized and multi-sized granular piles from the rising funnel. For the uniformly-sized granular pile, the particle diameter is equal to 1.4mm, while the particle diameter of the multi-sized granular pile is uniformly distributed and varies from 1.35-1.65mm. At the end of the piling process and after the granular piles settled down and reached a steady state condition, the heights, angles of repose, and normal force distributions at the base of each pile were measured. The mono-sized pile height was 27mm, while the multi-sized was 26.98mm and they almost have the same angle of repose $\cong 20^{o}$. Figure 4 shows the velocity field in the mono-sized granular pile at two instants of time during the filling process. Figure 5 shows the normal force distributions on the base of the two granular piles.

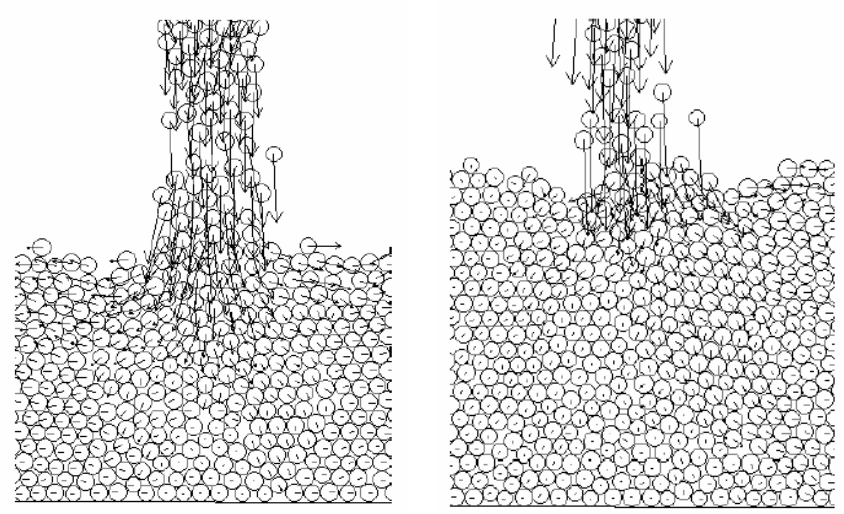

Figure 4. Velocity field of mono-sized granular piles during filling at 100s and 150s.

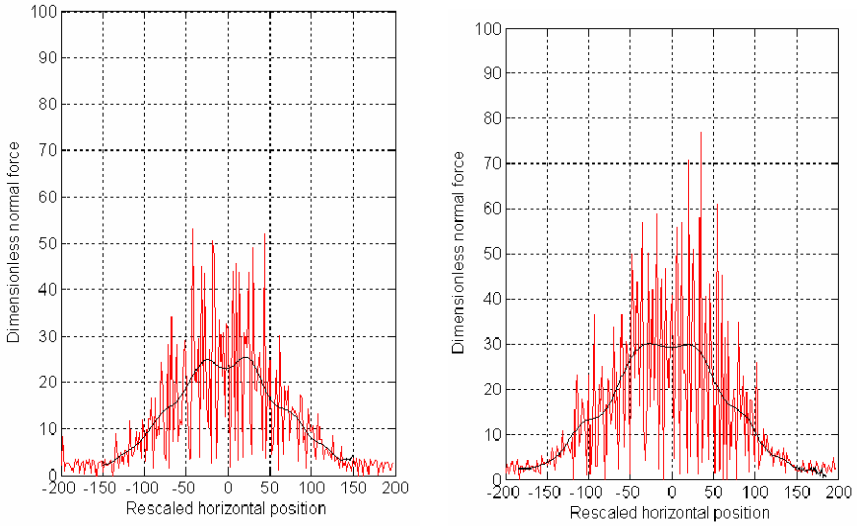

(a) (b)

Figure 5. The normal force distributions on the base of the two piles with different particle diameter: (a) 1.4mm (mono-sized) and (b) 1.35-1.65mm (multi-sized).

The results show the existence of a normal force local minimum at the centre of the base under the pile vertex. This agrees well with previous experimental results [1, 8, 12, 13]. This also means that constructing a granular pile with a rising localized source leads to a local stress minimum under the apex of a granular pile. Moreover, it has been observed that the normal force at the apex surrounding region of the mono-sized pile attains values less than that for the multi-sized pile. For multi-sized granular piles, the normal force dip under apex is greater than that of the mono-sized pile. Force chains within the granular piles, which are constructed with rising localized source are oriented in the direction of the slopes. Therefore, in this case, there are arch like structures, which shield the centre from some of the bulk weight and cause void above the centre of the pile base.

3.2. Influence of pile height

A series of test simulations were conducted to investigate the effect of the pile height on the normal force on the base of a granular pile. Mono-sized and multi-sized granular piles with different heights were constructed from the rising funnel. Mono-sized piles were constructed with particles of diameter 1.4mm, and the heights range from 15.87mm to 25.4mm. Figure 6 shows the normal force distributions under the four mono-sized piles with different height. For all piles, a local minimum under the apex was observed in the normal force profile. Since the avalanches occur left and right by turns during the piling process, the dip does not exactly occur under the apex, but rather it fluctuates in the horizontal direction along the pile base [8]. For the small size granular piles, the normal force distribution on the base seems to be smoother than that for the large piles.

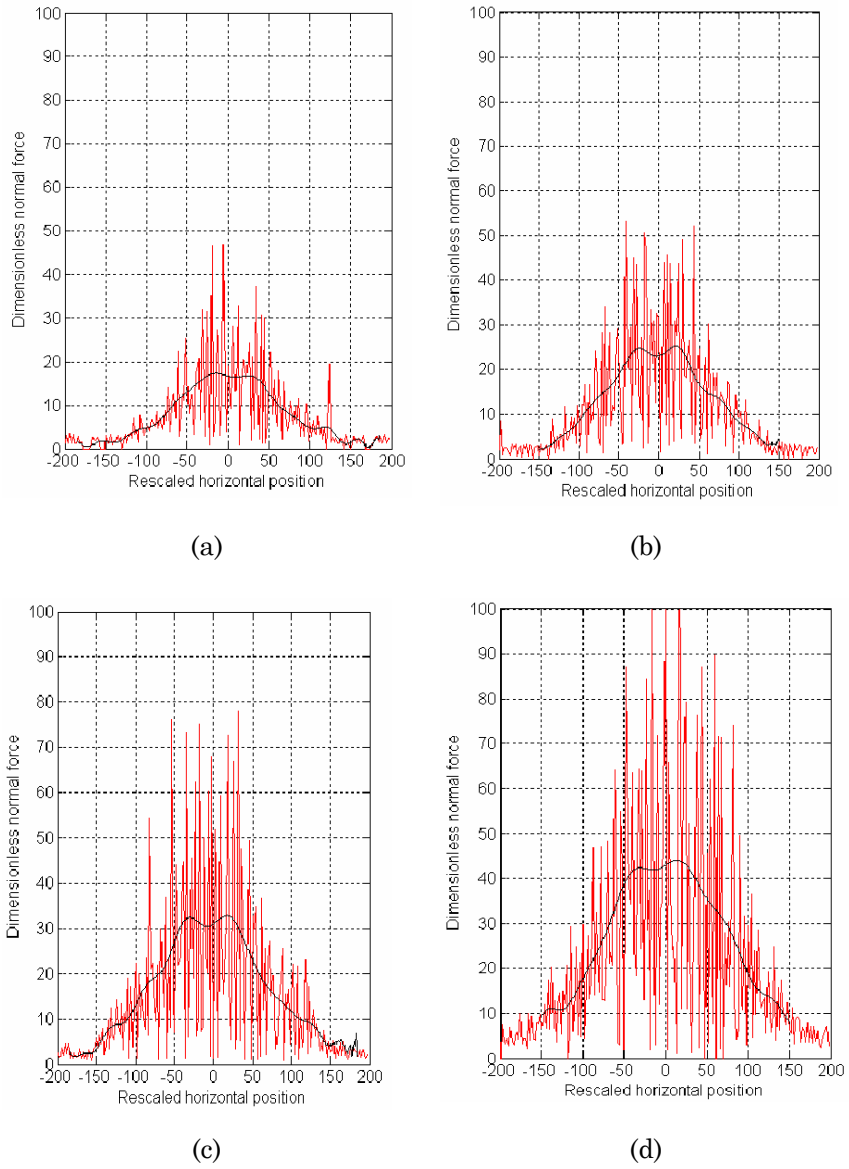

Figure 6. The normal force distribution on the base of mono-sized granular piles with different heights: (a) 13mm, (b) 17mm, (c) 20mm, and (d) 27mm.

The same observations were obtained for the multi-sized piles with different heights. The distributions of the normal forces under the piles are given in Figure 7. For piles with small heights, the profiles of the normal force distributions are smoother than that for the piles with large heights. It can be clearly observed that the fluctuations in the normal force distributions for the high multi-sized granular piles are more significant than that for the small multi-sized piles. This can be attributed to the particles at the bottom of the granular pile, which can be the primary members of force chains. These particles bear the majority of the pile weight. Hence, the fluctuations in the normal force distributions for the higher piles are larger than that for the smaller piles.

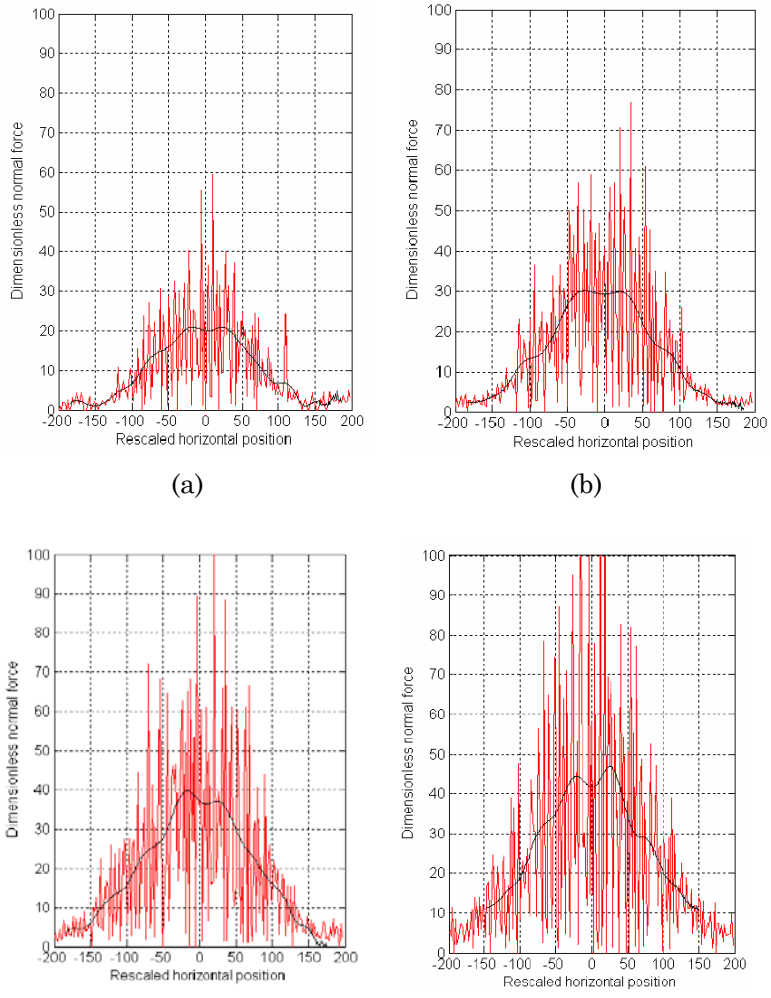

Figure 7. The normal force distribution on the base of multi-sized granular piles with different heights: (a) 15mm, (b) 19mm, (c) 23mm, and (d) 29mm.

Figure 8 shows the relationship between the normal force under the apex and the height for mono-sized and multi-sized granular piles. The results show that the normal force under the apex is proportional to the pile height in both cases.

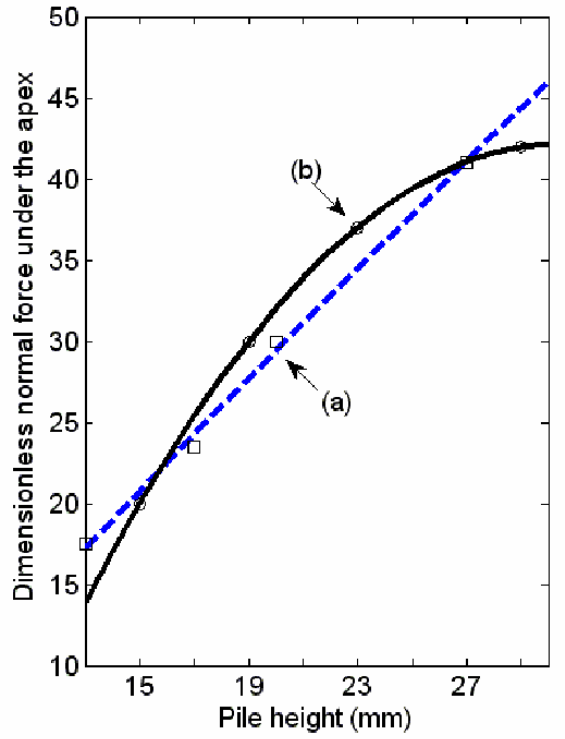

Figure 8. The relationship between the normal force under the apex and the height of a granular pile with different particle diameters: (a) 1.4mm (mono-sized) and (b) 1.3-1.7mm (multi-sized).

4. Conclusion

In this paper, a mathematical model and numerical techniques have been developed to study the dynamic process of the sandpile formation. The numerical simulation results show that the developed model and method are capable of capturing the phenomena of the existence of a local minima of the normal stress at the center point of the base of the sand-pile. The results show that particle size distribution also has significant effect on the normal stress acting on the base of the sand-pile. For multi-sized granular piles, the normal stress acting on the central does not increase linearly with respect to the height of the sand-pile; and the rate of increase decreases as the height increases.

References

[1] J. Baxter, U. Tüzün, J. Burnell and D. M. Heyes, Granular dynamics simulations of two-dimensional heap formation, Phys. Rev. E 55 (1997), 3546-3554.

[2] F. Cantelaube and J. D. Goddard, Elastoplastic Arching in 2D Heaps, Powders and Grains, Proc. 3rd Int. Conf., Durham, NC, USA, 18-23 May 1997 (Eds. R. P. Behringer and J. T. Jenkins), pp. 303-306, Rotterdam: Balkema, 1997.

[3] M. E. Cates and J. P. Wittmer, Stress propagation in sand, Physica A: Stat. Theo. Phys. 249(1-4) (1998), 276-284.

[4] M. E. Cates, J. P. Wittmer, P. Claudin and J.-P. Bouchaud, Development of stresses in cohesionless poured sand, Phil. Trans. R. Soc. A 356 (1998), 2535-2561.

[5] P. A. Cundall and D. L. Strack, A discrete numerical model for granular assemblies, Geotechnique 29 (1979), 47-65.

[6] T. Elperin and A. Vikhansky, Stress distribution in sandpiles: A variational approach, Physica A: Stat. Theo. Phys. 260(1-2) (1998), 201-217.

[7] J. M. Hill and G. M. Cox, The force distribution at the base of sandpiles, Developments in Theoretical Geomechanics, The John Booker Memorial Symposium, (Eds. D. W. Smith and J. P. Carter) (2000), 43-61.

[8] Shio Inagaki et al., Pressure distribution under a two-dimensional sandpile, (Mathematical Aspects of Complex Fluids II), RIMS Kokyuroku 1184 (2001), 140-151.

[9] Shio Inagaki and J. T. Jenkins, Stress and strain in flat piling of disks, J. Phys. Soc. Jpn. 73(44) (2004), 926-931.

[10] E. Li and D. F. Bagster, A new block model of heaps, Powder Tech. 63(3) (1990), 277-283.

[11] W. McBride, Base pressure measurements under a scale model stockpile, Partic. Sci. Tech. 24 (2006), 59-70.

[12] J. Smid and J. Novosad, Pressure distribution under heaped bulk solids, Ind. Chem. Eng. Symp. 63 (1981), D3/V/1-D3/V/12.

[13] L. Vanel, D. W. Howell, D. Clark, R. P. Behringer and E. Clement, Memories in sand: Experimental tests of construction history on stress distributions under sandpiles, Phys. Rev. E 60 (1999), R5040.

■